

RESEARCH ARTICLE

# Quantitative analysis of yield and soil water balance for summer maize on the piedmont of the North China Plain using AquaCrop

Jingjing WANG<sup>1,2</sup>, Feng HUANG<sup>1,2</sup>, Baoguo LI (✉)<sup>1,2</sup>

<sup>1</sup> Department of Soil and Water Science, College of Resources and Environment, China Agricultural University, Beijing 100193, China

<sup>2</sup> Key Laboratory of Arable Land Conservation (North China), Ministry of Agriculture, Beijing 100193, China

**Abstract** The North China Plain (NCP) is a major grain production area in China, but the current winter wheat-summer maize system has resulted in a large water deficit. This water-shortage necessitates the improvement of crop water productivity in the NCP. A crop water model, AquaCrop, was adopted to investigate yield and water productivity (*WP*) for rain-fed summer maize on the piedmont of the NCP. The data sets to calibrate and validate the model were obtained from a 3-year (2011–2013) field experiment conducted on the Yanshan piedmont of the NCP. The range of root mean square error (*RMSE*) between the simulated and measured biomass was 0.67–1.25 t·hm<sup>-2</sup>, and that of relative error (*RE*) was 9.4%–15.4%, the coefficient of determination (*R*<sup>2</sup>) ranged from 0.992 to 0.994. The *RMSE* between the simulated and measured soil water storage at depth of 0–100 cm ranged from 4.09 to 4.39 mm; and *RE* and *R*<sup>2</sup> in the range of 1.07%–1.20% and 0.880–0.997, respectively. The *WP* as measured by crop yield per unit evapotranspiration was 2.50–2.66 kg·m<sup>-3</sup>. The simulated impact of long-term climate (i.e., 1980–2010) and groundwater depth on crop yield and *WP* revealed that the higher yield and *WP* could be obtained in dry years in areas with capillary recharge from groundwater, and much lower values elsewhere. The simulation also suggested that supplementary irrigation in areas without capillary groundwater would not result in groundwater over-tapping since the precipitation can meet the water required by both maize and ecosystem, thus a beneficial outcome for both food and ecosystem security can be assured.

**Keywords** AquaCrop, summer maize, soil water balance, water productivity

## 1 Introduction

The North China Plain (NCP) is one of the most important grain production areas in China and home to more than 300 million people<sup>[1–5]</sup>. It produces approximately one-fourth of the country's grain output with only 5.57% of national water resources, and is currently experiencing intense water shortages and related environmental problems<sup>[6,7]</sup>. Water and crop production interact with each other: grain production consumes enormous amounts of water while water limits crop production<sup>[8–11]</sup>. The double-cropping winter wheat (*Triticum aestivum*) and maize (*Zea mays*) is the dominant farming system in most parts of the NCP, with these cereals accounting for the vast majority of the gross crop output (i.e., more than 90%)<sup>[1,12]</sup>. Crop growth relies heavily on irrigation because both the amount (400–600 mm) and the timing (mostly occurring in summer monsoons) of annual precipitation are not appropriate to support the winter wheat-summer maize (WW-SM) cropping system. Current groundwater withdrawn for irrigation far exceeds the natural recharge rates of the aquifers, resulting in a rapid fall in the groundwater table<sup>[13]</sup>. Therefore, developing a water-efficient cropping system is the key to improving crop water productivity and developing water-saving agriculture in this region<sup>[7]</sup>. Much evidence suggests that the changes in rainfall regimes are the most direct and important factor responsible for water shortage and necessitate irrigation. More specifically, the annual rainfall, days of rainfall and daily rainfall in the NCP have all declined since the 1950s<sup>[6,14–16]</sup>. In light of these findings, it is vital to further investigate the relationships between crop growth, yield, and water consumption of summer maize that is primarily relied on rain-fed, with the objective of obtaining beneficial outcomes for improving crop water productivity (*WP*), gross crop outputs and feeding a growing population.

Received September 30, 2015; accepted October 23, 2015

Correspondence: [libg@cau.edu.cn](mailto:libg@cau.edu.cn)

In contrast to field experimental studies, crop models require fewer resources and can provide information faster. Crop modeling can also complement field experiments<sup>[17–20]</sup>. As an alternative to crop water production functions, by considering various environment conditions and management practices, crop models can provide rapid estimates of water-limited crop growth and yield<sup>[19]</sup>. However, most of these models require detailed parameters (which are usually difficult to obtain) which describe plant growth behavior (APSIM<sup>[21]</sup>; CERES<sup>[22]</sup>), or make use of empirical functions (CROPWAT<sup>[23]</sup>), or tend to be technically demanding and input-intensive and not easily adopted by practitioners<sup>[24,25]</sup>. Thus the wide applications of these models are limited.

To resolve these limitations, the Food and Agriculture Organization of the United Nations (FAO) has developed AquaCrop<sup>[26]</sup> as a model that seeks a balance between simplicity, accuracy and robustness, which is user-friendly and practitioner-oriented and requires a relatively small number of input parameters<sup>[27]</sup>. AquaCrop, as a crop water productivity simulation model, was first released in January 2009 (Version 3)<sup>[28–30]</sup> and the current version 4.0 was released in August 2012<sup>[31]</sup>. The global applicability of AquaCrop is dependent on its being tested in a diverse environment under differing soil conditions, crops, agronomic practices, and climatic conditions<sup>[32,33]</sup>. For example, the calibration and evaluation of the performance of AquaCrop has been carried out for quinoa<sup>[34]</sup>, wheat<sup>[35–39]</sup>, sorghum<sup>[40]</sup>, maize<sup>[28,41–46]</sup>, potato<sup>[32,47]</sup>, and cabbage<sup>[48,49]</sup>.

Previous studies have demonstrated that AquaCrop is able to accurately simulate crop canopy cover, biomass yield and grain yield in diverse environments and under a variety of meteorological conditions and management practices. However, the quantification of soil water balance and rain-fed crop evapotranspiration in soil-plant-atmosphere continuum has rarely been reported with AquaCrop. Therefore, the objectives of the current study are (1) to test the performance and applicability of AquaCrop for the rain-fed summer maize through calibrating and validating a data set obtained from a three-year field experiment conducted in the piedmont of the NCP, and (2) to investigate responses of crop yield and *WP* to long-term climatic factors and groundwater depth. The study will provide guidelines to explore and evaluate alternative management practices that may improve *WP* and achieve more efficient water use for summer maize crops in the NCP piedmont.

## 2 Materials and methods

### 2.1 Experimental site

The field experiments were conducted in three consecutive years (2011, 2012, and 2013) in the piedmont of Yanshan

Mountain, Shangzhuang Experimental Station (116°10' E, 40°08' N) of China Agricultural University, Beijing, China. The depth of groundwater table is relatively shallow (1.0–1.5 m). The soil type at the study site is a calcareous alluvial fluvo-aquic soil with a loamy silt texture. The site belongs to warm temperate zone with a continental monsoon climate, which typically has a cold, dry winter and hot, humid summer. Annual mean precipitation is 596 mm, with more than 82% occurring in three monsoon months from June to August. The annual mean temperature is 12.2°C, with the maximum 41.9°C recorded in July and the minimum of –27.4°C in January (1951–2010). The typical cropping system is WW-SM, with October to June for winter wheat and June to October for summer maize.

### 2.2 AquaCrop model description

The AquaCrop model<sup>[26,50]</sup> was established on the basic relationship of yield response to water, which was first developed by Doorenbos and Kassam<sup>[51]</sup> and has evolved to a daily-step, process-based crop growth model with limited complexity (Eq. 1),

$$\left(\frac{Y_x - Y_a}{Y_x}\right) = k_y \left(\frac{ET_x - ET_a}{ET_x}\right) \quad (1)$$

where  $Y_x$  and  $Y_a$  are the maximum and actual yield,  $ET_x$  and  $ET_a$  are the maximum and actual evapotranspiration, and  $k_y$  is the proportionality factor between relative yield loss and relative reduction in evapotranspiration.

AquaCrop is based on a water-driven growth module, in which plant transpiration is converted into biomass through a water productivity parameter. Hence, the conceptual equation at the core of the AquaCrop growth module is,

$$B = WP \times \Sigma T \quad (2)$$

where  $T$  is the crop transpiration (mm);  $B$  is crop biomass;  $WP$  is the water productivity ( $\text{kg} \cdot \text{m}^{-3}$ ) (biomass per unit of cumulative transpiration), which tends to be constant for a given climatic condition<sup>[52–54]</sup>. Details of the simulated processes of AquaCrop are provided in a series of three papers<sup>[28–30,50]</sup>, in the Irrigation and Drainage Paper No. 66<sup>[55]</sup>, and in the reference manual<sup>[31]</sup> that is updated regularly.

### 2.3 Soil water balance parameters description

The AquaCrop model is a water-driven dynamic model that ties biomass production to transpiration, so soil water balance is a critical component<sup>[31]</sup>. To accurately describe the retention, movement, and uptake of water in the soil profile throughout the growing season, AquaCrop divides a soil profile into small fractions. A soil profile is divided into soil compartments with thickness  $\Delta z$  (10 cm by default for each layer)<sup>[29]</sup>. The water balance<sup>[31,56]</sup> for a given soil

profile with certain depth in AquaCrop can be expressed as,

$$\Delta SW = P + U + I - R - D - E - T \quad (3)$$

where  $\Delta SW$  is the change in the soil water storage from 0 to 100 cm during a given period (mm);  $I$  is irrigation (mm) ( $I = 0$  because the summer maize in this study is rain-fed);  $P$  is precipitation (mm);  $R$  is runoff (mm);  $D$  is drainage (mm);  $U$  is capillary rise (mm);  $E$  is evaporation (mm);  $T$  is transpiration (mm).

Soil water content was measured by the oven dry method. Three replications of soil samples from different layers (0–5, 5–10, 10–20, 20–40, 40–60, 60–80, and 80–100 cm each) were collected during seedling (Jul. 18, 2012 and Jul. 4, 2013), jointing (Jul. 24, 2012 and Jul. 17, 2013), silking (Aug. 2, 2011, Aug. 14, 2012, and Aug. 7, 2013), grain filling (Aug. 29, 2011, Aug. 31, 2012, and Aug. 22, 2013), milky ripeness (Sep. 22, 2011, Sep. 12, 2012, and Sep. 12, 2013), and maturity (Oct. 10, 2011, Oct. 5, 2012, and Oct. 5, 2013). The soil water storage ( $\Delta SW$ ) within a given depth of soil profile was calculated using soil water content. Precipitation ( $P$ ) was obtained from the China meteorological data sharing service system ([http://www.cma.gov.cn/cams\\_kxxy/qky\\_kxxy\\_index.htm](http://www.cma.gov.cn/cams_kxxy/qky_kxxy_index.htm)). The current version 4.0 of the AquaCrop model estimates the amount of rainfall lost by surface runoff ( $R$ ) with the Curve Number (CN) method by the US Soil Conservation

Service<sup>[57–59]</sup>. The specified daily CN values in AquaCrop was determined by the antecedent moisture class (AMC) which was derived from the rainfall of the preceding 5 days, and the CN value varied with the land use, management practices, and saturated hydraulic conductivity of the top soil layer<sup>[31]</sup>. The drainage ( $D$ ) was calculated following<sup>[60–62]</sup>,

$$D = 1000 \frac{\Delta \theta}{\Delta t} \Delta z \Delta t \quad (4)$$

where  $\Delta \theta / \Delta t$  denotes changes in soil water content during time step  $\Delta t$  ( $\text{m}^3 \cdot \text{m}^{-3} \cdot \text{d}^{-1}$ );  $\Delta t$ , the time step (1 d);  $\Delta z$ , the thickness of the draining soil profile (m).

Capillary rise ( $U$ ) is calculated following Janssens<sup>[63]</sup>. The relationship between capillary rise and the depth of the groundwater table is given by the exponential equation,

$$U = \exp\left(\frac{\ln(z) - b}{a}\right) \quad (5)$$

where  $U$  is the expected capillary rise ( $\text{mm} \cdot \text{d}^{-1}$ ),  $z$  is the depth (m) of the water table below the soil surface;  $a$  and  $b$  are parameters specific for the soil type and its hydraulic characteristics, and they are estimated based on the data listed in Table 1 and Table 2.

AquaCrop partitioned evapotranspiration ( $ET$ ) into crop transpiration ( $T$ ) and soil evaporation ( $E$ ) based on a simple canopy growth and senescence module to estimate  $T$  and

**Table 1** Basic soil physical and chemical properties at experimental site (Shangzhuang Experimental Station, 116°10'E, 40°08'N)

Depth/cm	Texture	Particle size composition/%			BD/(g·cm <sup>-3</sup> )	pH
		Sand	Silt	Clay		
0–5	Sandy loam	54.63	34.29	11.08	1.48	8.07
5–10	Sandy loam	60.19	28.60	11.21	1.47	8.05
10–20	Sandy loam	56.90	32.85	10.25	1.49	8.00
20–40	Loam	52.13	38.18	9.69	1.62	8.02
40–60	Sandy loam	61.56	31.75	6.69	1.62	8.02
60–80	Loam	52.86	39.11	8.03	1.59	7.68
80–100	Loam	50.99	41.27	7.73	1.53	7.49

Note: BD, bulk density; pH (soil: water = 1: 2.5); classification of soil texture accorded to USDA.

**Table 2** Soil hydraulic parameters

Depth/cm	$\theta_r$ /(cm <sup>3</sup> ·cm <sup>-3</sup> )	$\theta_f$ /(cm <sup>3</sup> ·cm <sup>-3</sup> )	$\theta_s$ /(cm <sup>3</sup> ·cm <sup>-3</sup> )	$a$	$n$	$K_s$ /(cm·d <sup>-1</sup> )
0–5	0.093	0.261	0.458	0.09	1.29	55.034
5–10	0.073	0.236	0.418	0.08	1.33	53.892
10–20	0.070	0.252	0.440	0.10	1.32	61.318
20–40	0.077	0.259	0.393	0.04	1.40	65.938
40–60	0.069	0.249	0.390	0.02	1.56	99.382
60–80	0.073	0.279	0.440	0.03	1.37	81.022
80–100	0.064	0.245	0.437	0.01	1.84	83.606

Note:  $\theta_r$ , the residual water content;  $\theta_f$ , field capacity;  $\theta_s$ , the saturated water content;  $K_s$ , the saturated hydraulic conductivity;  $a$  and  $n$  are the parameters of the soil water retention curve in the Van Genuchten Eq. 1980.

distinguish it from  $ET^{[30]}$ . The partitioning of  $ET$  into  $T$  and  $E$  rules out the confounding effect of the nonproductive water consumption because  $E$  is a significant factor during incomplete ground cover. AquaCrop uses canopy cover ( $CC$ ) instead of leaf area index ( $LAI$ ) to separate  $E$  from  $ET$  according to the extent of green  $CC$ , aboveground biomass production in relation to  $T$ .  $T$  is given by,

$$T = \sum_{\text{top}}^{\text{bottom}} 1000(K_{S_i} S_{x,i}) dz_i \leq \overline{K_{S_{\text{root zone}}}} K_{C_{T_r}} ET_0 \quad (6)$$

where  $K_{S_i}$  is water stress factor (dimensionless) for soil water content  $\theta_i$  ( $\text{m}^3 \cdot \text{m}^{-3}$ ) at soil depth  $i$ ;  $S_{x,i}^{[64-66]}$  is maximum root extraction rate ( $\text{m}^3 \cdot \text{m}^{-3} \cdot \text{d}^{-1}$ ) at soil depth  $i$ ;  $dz_i$  is the thickness of the soil compartment (m);  $\overline{K_{S_{\text{root zone}}}}$  is the average soil water stress in the root zone induced by a shortage or an excess of water and/or aeration stress;  $K_{C_{T_r}}$  is the coefficient for crop transpiration;  $ET_0$  is reference crop evapotranspiration ( $\text{mm} \cdot \text{d}^{-1}$ ). If the crop is free from any biotic and abiotic stress  $T$  will achieve the maximum  $T_0$ .

$E$  from soils takes place in two stages<sup>[67]</sup>, and the algorithm was based on Ritchie Method<sup>[68]</sup>,

$$E_{\text{stage I}} = (1 - CC^*) K_{e_x} ET_0 \quad (7)$$

$$E_{\text{stage II}} = K_r (1 - CC^*) K_{e_x} ET_0 \quad (8)$$

$$0 \leq K_r = \frac{\exp^{f_k W_{rel-1}}}{\exp^{f_{k-1}}} \leq 1 \quad (9)$$

where  $CC$  is canopy cover,  $(1 - CC^*)$  is the adjusted fraction of the non-covered soil surface<sup>[69,70]</sup>;  $K_{e_x}$  is maximum soil evaporation coefficient for fully wet and non-shaded soil surface, the default value is 1.10<sup>[71]</sup>;  $K_r$  is the evaporation reduction coefficient;  $f_k$  is a decline factor, the value of  $f_k$  depends on the hydraulic properties of soil and can be used to calibrate  $K_r$  (Table 2), which takes a value of 4<sup>[68]</sup>;  $W_{rel}$  is the relative water content of the soil layer through which water moves to the evaporating soil surface layer. When  $CC^* = 0$ ,  $E_{\text{stage I}} = E_0$ .

#### 2.4 AquaCrop model inputs

The required parameters for maize growth simulation by five major modules of AquaCrop (i.e., climate, crop, management, soil and initial conditions) were obtained first from Hsiao<sup>[28]</sup> and FAO<sup>[26]</sup>. Then, the measured data obtained from field experiment of summer maize at Shangzhuang Experimental Station of China Agricultural University in 2012 were incorporated into the model for the purpose of calibration. The simulation was run under conditions of no fertility or heat stress. Upon calibration, the experimental data obtained from 2011 and 2013 were used to validate the model.

#### 2.5 Climate data collection and analysis

AquaCrop requires daily values of minimum and maximum air temperature, precipitation, reference evapotranspiration ( $ET_0$ ), and the mean annual  $\text{CO}_2$  concentration in the atmosphere<sup>[29,30]</sup>. Meteorological variables, including temperature, humidity, wind speed, sunshine hours and net solar radiation, were obtained from the China meteorological data sharing service system ([http://www.cams.cma.gov.cn/cams\\_kxxy/qky\\_kxxy\\_index.htm](http://www.cams.cma.gov.cn/cams_kxxy/qky_kxxy_index.htm)). Beijing Weather Station was selected to represent the weather conditions at Shangzhuang Experimental Station of China Agricultural University.

The daily  $ET_0$  at Shangzhuang experimental station for the growing season from 2011 to 2013 were computed using a full set of data based on the FAO Penman-Monteith method as described in Allen<sup>[71]</sup> with the help of the  $ET_0$  calculator<sup>[26]</sup>. Daily weather data of sunshine hours, wind speed, relative humidity, and temperature and rainfall were obtained from BWS. Distributions for the daily precipitation, temperature variations and  $ET_0$  during the maize growing seasons (planting through physiological maturity) from 2011 to 2013 are shown in Fig. 1.

#### 2.6 Crop data collection and analysis

The days after planting (DAP) at emergence, maximum canopy cover, start of senescence, and physiological maturity were recorded. Plant samples from three plots were collected, mixed and oven-dried at 75°C to determine the aboveground biomass. Maize yield was determined by sampling an area of 5 m × 2 m at the maturity stage. The yields were reported at 14% moisture content.

Most of the crop parameters were either measured or estimated using the experiment data in 2012 (Table 3, Table 4). The normalized biomass water productivity ( $WP^*$ ) is one of the most important parameters in AquaCrop, the values of which are set as 13–18  $\text{g} \cdot \text{m}^{-2}$  for  $C_3$  species and 28–33  $\text{g} \cdot \text{m}^{-2}$  for  $C_4$  species like maize<sup>[30,72]</sup>. The local values were determined as 30.7  $\text{g} \cdot \text{m}^{-2}$  (Table 4) based on experimental data in 2012, following the procedure of Hsiao<sup>[28]</sup> and Heng<sup>[42]</sup>. In this study, the fertility levels, mulching and soil bunds were not considered in the management module.

#### 2.7 Soil data analysis

Three replications of soil samples at five different layers (0–20, 20–40, 40–60, 60–80, and 80–100 cm) were collected on October 7, 2012. The AquaCrop soil component allows up to five different horizons of variable depth and soil texture. For each horizon within the soil profile, AquaCrop requires saturated hydraulic conductivity ( $K_{\text{sat}}$ ) and volumetric water content at the

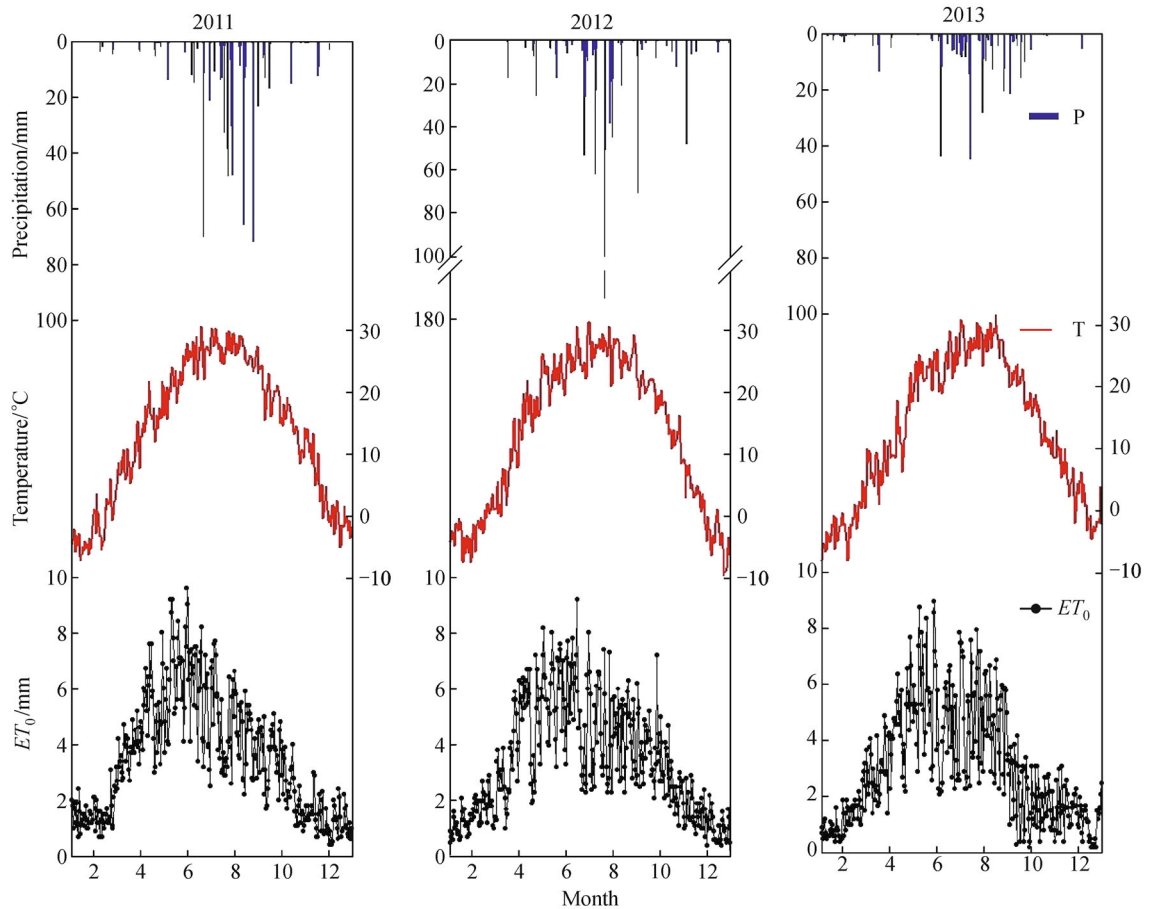


**Fig. 1** Daily trends in environmental conditions at the experimental site from 2011 to 2013. Meteorological data includes daily precipitation ( $P$ ); mean day time air temperature ( $T$ ); daily potential evapotranspiration ( $ET_0$ ).

**Table 3** Crop parameters used in AquaCrop model for summer maize simulation

Year	Planting date	Emergence	Max canopy	Senescence	Maturity	$CC_0/\%$	$CC_s/\%$	$CGC/\%$	$CDC/\%$
2011	June 25	6	54	86	108	0.39	92	16.6	13.7
2012	June 23	6	54	84	105	0.39	92	16.7	12
2013	July 1	6	59	80	97	0.36	92	15.2	13.8

Note:  $CC_0$ , canopy cover per seedling at 90% emergence;  $CC_s$ , maximum canopy cover;  $CGC$ , canopy growth coefficient per day;  $CDC$ , canopy decline coefficient per day; DAP, days after planting.

permanent wilting point ( $\theta_{pWP}$ ), field capacity ( $\theta_{FC}$ ), and saturation ( $\theta_{sat}$ )<sup>[29]</sup>.

Soil properties including bulk density, soil texture, soil water content, saturated hydraulic conductivity and pH at different depths were measured. Bulk density was measured with the oven dry method, using a sample size of 100 cm<sup>3</sup>. The saturated hydraulic conductivities ( $K_{sat}$ ) were measured with the constant-head method in the laboratory<sup>[73]</sup>. Soil water retention curves were developed

for the soil samples by the pressure plate method<sup>[74]</sup>, with the sand box apparatus for lower suctions (0, 0.5, 1.0, 2.0, 4.0, 6.0, and 8.0 kPa) and the pressure membrane-plate system for higher suctions (10, 30, 50, 100, 300, 500, and 1500 kPa) (Soil moisture Equipment Corp, Santa Barbara, CA). Major soil parameters were measured in 2012, including soil physical and chemical properties (Table 1) and soil hydraulic parameters (Table 2). The experimental site did not have any impervious or restrictive soil layer

**Table 4** Some relevant crop parameters used in the AquaCrop model for summer maize simulation

Parameters	Value	Units	Way of determination
Plant density	60606	Plants per hectare	M
Maximum effective rooting depth ( $Z_r$ )	1.00	m	E
Base temperature	8	°C	E
Cut-off temperature	30	°C	E
Crop coefficient when canopy is complete but prior to senescence ( $Kc_{Tx}$ )	1.03	–	D
Normalized crop water productivity ( $WP^*$ )	30.70	$g \cdot m^{-2}$	C
Reference harvest index ( $HI_0$ )	40	%	C
Leaf growth threshold ( $P_{exp, upper}$ )	0.14	–	D
Leaf growth threshold ( $P_{exp, lower}$ )	0.72	–	D
Leaf growth stress coefficient curve shape	2.90	–	D
Stomatal conductance threshold ( $P_{sto, upper}$ )	0.69	–	D
Stomata stress coefficient curve shape	6.00	–	D
Senescence stress coefficient ( $P_{sen, upper}$ )	0.69	–	D
Senescence stress coefficient curve shape	2.70	–	D
Curve number (CN)	65	–	C
Readily evaporable water (REW)	8	mm	C

Note: C, calibrated; D, default; E, estimated; M, measured.

influencing root expansion.

## 2.8 Water productivity

Crop water productivity was defined from a physiological perspective as the ratio of biomass to consumed water<sup>[75–78]</sup>. Thus, for maize water use efficiency is described by the following equation,

$$WP = \frac{Y}{ET} \quad (10)$$

where  $Y$  is grain yield ( $kg \cdot hm^{-2}$ ), and  $ET$  (mm) is the evaporation of water from the soil surface plus transpiration from the crop.

## 2.9 Date analysis

Summer maize aboveground biomass, yield and soil water storage in AquaCrop were calibrated using the measured data set of 2012, and validated using the 2011 and 2013 measured data sets. The root mean square error ( $RMSE$ ), coefficient of determination ( $R^2$ ), and the range of relative error ( $RE$ )<sup>[79]</sup> were used as the error statistics to evaluate both calibration and validation results were calculated as,

$$RMSE = \sqrt{\frac{\sum_{i=1}^n (S_i - O_i)^2}{n}} \quad (11)$$

where  $S_i$  and  $O_i$  refer to simulated and measured values in the same units of the study variables, respectively, and  $n$  is the number of observations. The unit for  $RMSE$  is the same

as that for  $S_i$  and  $O_i$ , and a model's fit improves as  $RMSE$  approaches zero.

$R^2$  was calculated using the following equation,

$$R^2 = \left[ \frac{\sum (O_i - \bar{O})(S_i - \bar{S})}{\sqrt{\sum (O_i - \bar{O})^2 \sum (S_i - \bar{S})^2}} \right]^2 \quad (12)$$

where  $S_i$  and  $O_i$  are simulated and measured values, respectively,  $\bar{S}$  is the mean of  $S$  and  $\bar{O}$  is the mean of  $O$ .

$RE$ <sup>[80]</sup> between a simulated ( $S$ ) and measured ( $O$ ) value is simple and when expressed as a percentage easy to interpret,

$$RE\% = \left| \frac{S - O}{O} \right| \times 100 \quad (13)$$

## 3 Results

### 3.1 Above-ground biomass and yield

In AquaCrop, the crop response to environmental conditions and to root-zone water balance is captured through water stress indices. The plentiful growing-season rainfall in 2011, 2012, and 2013 met the maize requirement for water. Hence, the simulated biomass and yield matched fairly well with the actual values in all three years. The cumulative biomass production increased linearly with the

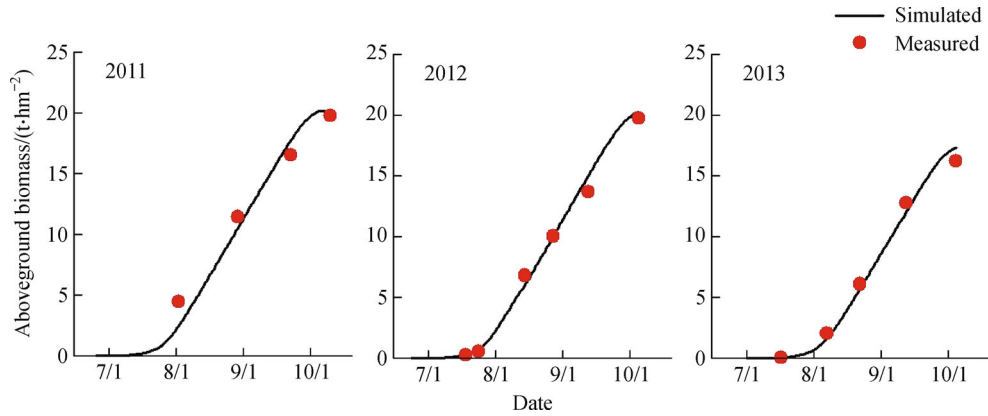


**Fig. 2** Simulated and measured above ground biomass dynamics summer maize in 2011, 2012, and 2013

development and growth of maize (Fig. 2). The calibrated *RMSE*, *RE*, and *R*<sup>2</sup> were 0.68 t·hm<sup>-2</sup>, 9.39% and 0.994, respectively. The data in the year 2011 and the year 2013 were used to validate the model, with the *RMSE* being 1.25 and 0.67 t·hm<sup>-2</sup>, respectively; *RE* being 15.38% and 13.37%, respectively; *R*<sup>2</sup> being 0.994 and 0.992, respectively. The *RE* of the simulated yield for the two individual years was below 9% (Table 5). In general, the simulated biomass and yield corresponded well with the measured ones.

**3.2 Soil water content and water storage**

Water content in the soil profile varied considerably due to variations in precipitation, *ET* and the capillary recharge from ground water. The soil volumetric water contents during the summer maize growing season are presented in Fig. 3. The majority of precipitation occurred from late June to early August during the growth seasons, with the most intense rainfall events concentrated between mid-July and early-August, hence the soil volumetric water content increased with soil depth for the years 2011–2013. The time-series changes of soil volumetric water content were due largely to rainfall events. This was further

**Table 5** Comparison of the simulated and measured maize yields from 2011 to 2013

Year	Comparison	Yield/( t·hm <sup>-2</sup> )
2011	Simulated	9.19
	Measured	9.54
	<i>RE</i> /%	3.67
2012	Simulated	8.14
	Measured	8.78
	<i>RE</i> /%	7.29
2013	Simulated	6.94
	Measured	6.38
	<i>RE</i> /%	8.78

Note: *RE* is the relative error.

illustrated by the case in 2012, when there were six heavy rains from 6 to 22 July, 2012 (13 to 29 DAP). For instance, the high rainfall on 21 and 22 July (200 mm), which was a 60-year record, led to a remarkable increase of soil volumetric water content in the 0–40 cm layer. However, during the hot and dry period from 15 to 31 August (50 to 70 DAP), soil volumetric water content decreased

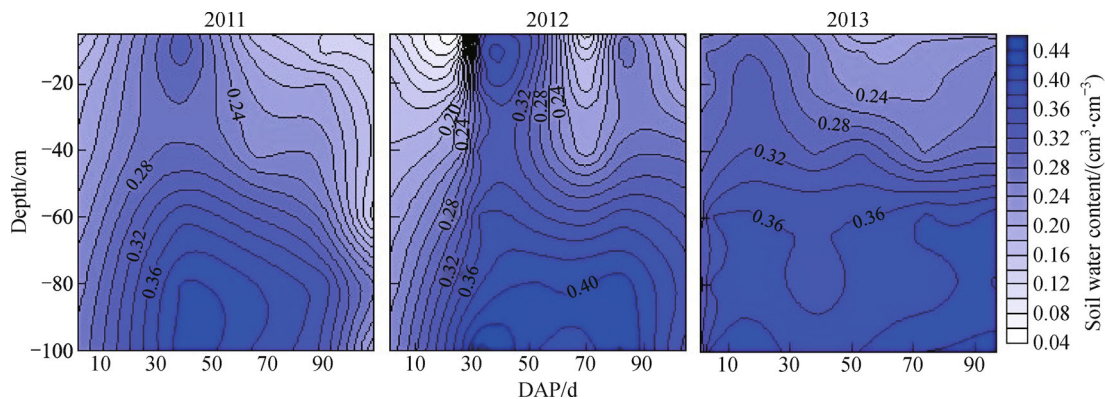


**Fig. 3** Contour map of soil water content in 0–100 cm soil profile in 2011, 2012, and 2013

markedly, especially in the upper 20 cm. There was no obvious change in the lower 40 cm of soil depth due to less  $E$  and more capillary recharge at such depths. Similar situation also occurred in the years 2011 and 2013.

The simulated soil water storage values at each 10 cm layer down to 100 cm were aggregated into 0–20 cm, 20–40 cm, and 0–100 cm layers, and agreed well with the measured values (Fig. 4, Table 6). The relative larger deviation from field measurement of simulated water storage in the upper layers (i.e., 0–20 cm and 20–40 cm) may be attributed to the upper layer effect (Table 6). Like biomass and yield, the measured soil water storage in 2012 was used to calibrate, and in 2011 and 2013 to validate, the model. The modeling performance indicators, i.e.,  $RMSE$ ,

$RE$ , and  $R^2$  (Table 6), suggested that the simulation results were acceptable.

### 3.3 Soil water balance and water productivity

The daily potential and actual  $E$ ,  $T$ , and  $ET$  were compared for 2011, 2012, and 2013 (Fig. 5). During the seedling stage, the actual  $E$  was smaller than potential  $E$ , and there were no differences between actual  $T$  and potential  $T$ . Since maize has strong drought tolerance at the seedling stage, and soil water content was greater than 60% of field capacity in the 0–20 cm soil layer, no water stress was observed. Water requirements increased at the jointing and anthesis stages. The roots of maize were distributed mainly

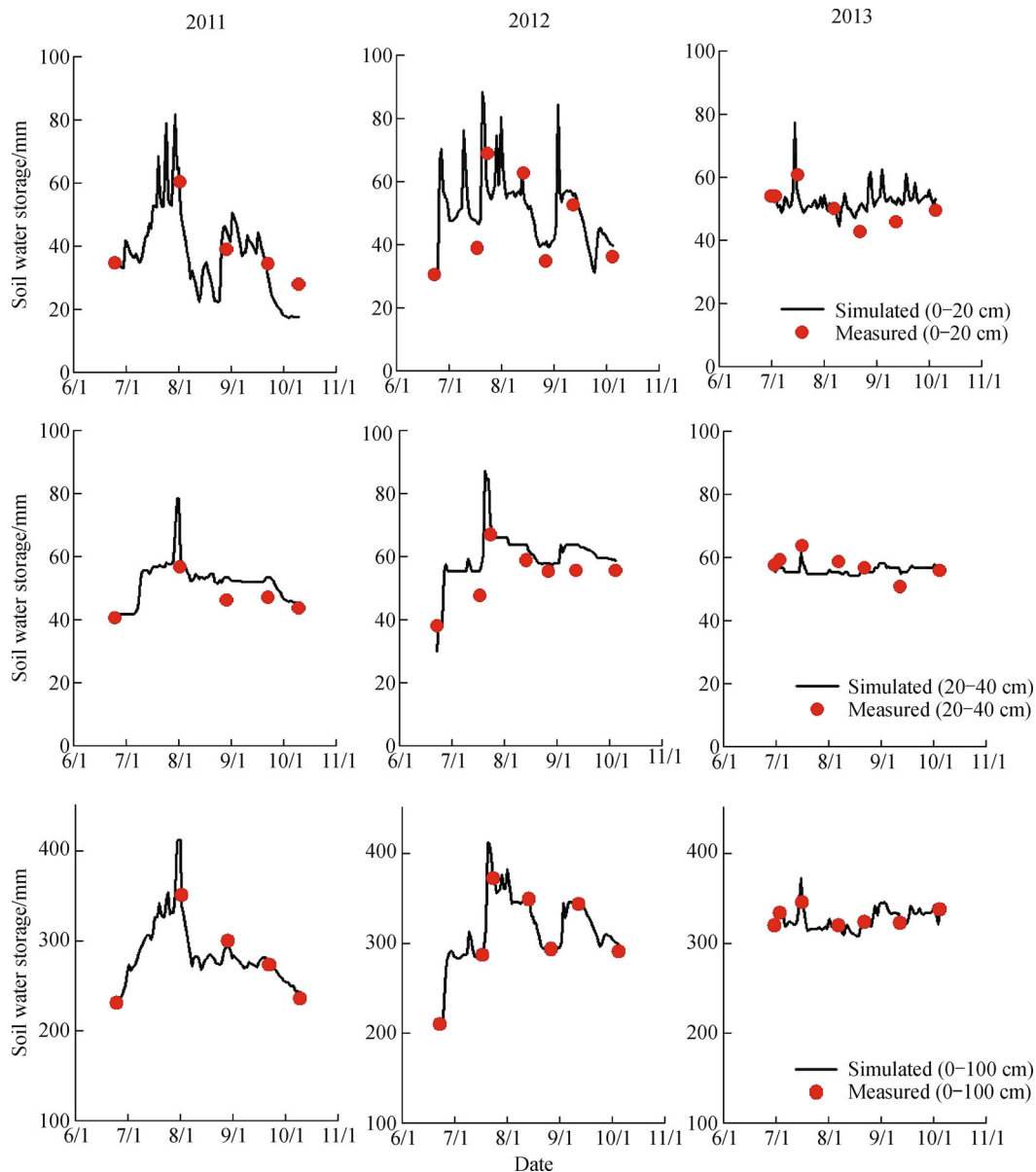


**Fig. 4** Comparison of modeled with observed soil water storage in 0–20 cm, 20–40 cm, and 0–100 cm for summer maize cropping seasons in 2011, 2012, and 2013

**Table 6** Comparison of the simulated and measured the soil water storage in the 0–20 cm, 20–40 cm, and 0–100 cm layers for the years from 2011 to 2013

Depth/cm	2011			2012			2013		
	RMSE/mm	RE/%	$R^2$	RMSE/mm	RE/%	$R^2$	RMSE/mm	RE/%	$R^2$
0–20	7.56	15.88	0.651	7.04	13.56	0.853	4.93	8.03	0.714
20–40	6.08	12.40	0.823	5.47	9.40	0.881	2.86	4.47	0.609
0–100	4.38	1.20	0.986	4.09	1.07	0.997	4.39	1.14	0.880

Note: RMSE, the root mean square error; RE, the relative error;  $R^2$ , the coefficient of determination.

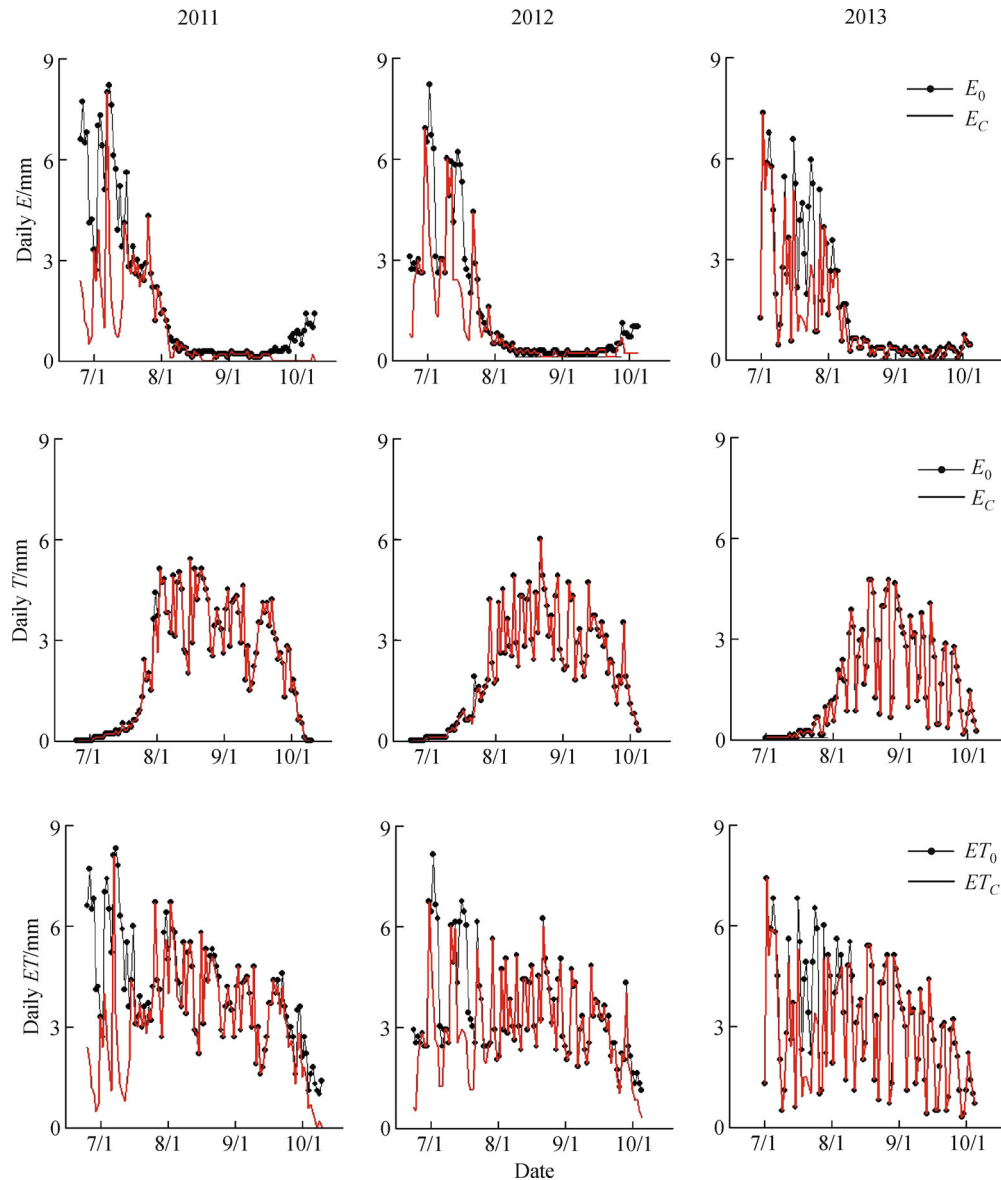


**Fig. 5** Daily potential evaporation ( $E_0$ ) and actual evaporation ( $E_C$ ), daily potential transpiration ( $T_0$ ) and actual transpiration ( $T_C$ ), daily potential evapotranspiration ( $ET_0$ ) and actual evapotranspiration ( $ET_C$ ) in 2011, 2012, and 2013

in the 0–40 cm soil layer. This was probably due to high-intensity rainfall, relative coarse soil texture (sandy loam), and the fact that water deficit occurred at the soil surface. The soil water content in the 10–40 cm soil layer was greater than 70% of field capacity, therefore, there was no

water stress during these stages. From grain filling to maturity,  $T$  was the dominant component in water consumption. There was no water stress observed because water content was larger than 75% of field capacity in the 10–40 cm soil layer.

Figure 6 shows the relationship between the ratio of actual daily  $ET$  to the potential daily  $ET$  ( $ET_C/ET_0$ ) and the precipitation for the years 2011 to 2013. During the early growth period, the maize canopy was not yet well established, and large areas of soil surface were left bare, resulting in a high proportion of  $E$  in  $ET$ .  $ET_C/ET_0$  fluctuated greatly in the case of low rainfall. With maize growth, the canopy covered much of the soil surfaces and consequently  $T$  became the major component of actual  $ET$ . There was no water stress during the middle and later

periods as could be seen by comparing actual crop  $T_C$  and potential  $T_0$  (Fig. 5). During these periods,  $ET_C/ET_0$  was relatively stable and close to 1. In the later stages, the canopy cover area decreased gradually with the senescence and abscission of leaves.  $ET_C/ET_0$  decreased because of the lower rainfall in 2011 and 2012, but  $ET_C/ET_0$  remained stable in 2013 due to the higher rainfall.

The daily water balance, including soil water storage, runoff, deep percolation, upward capillary movement,  $E$  and  $T$ , was also simulated (Table 7). Most of the rainfall

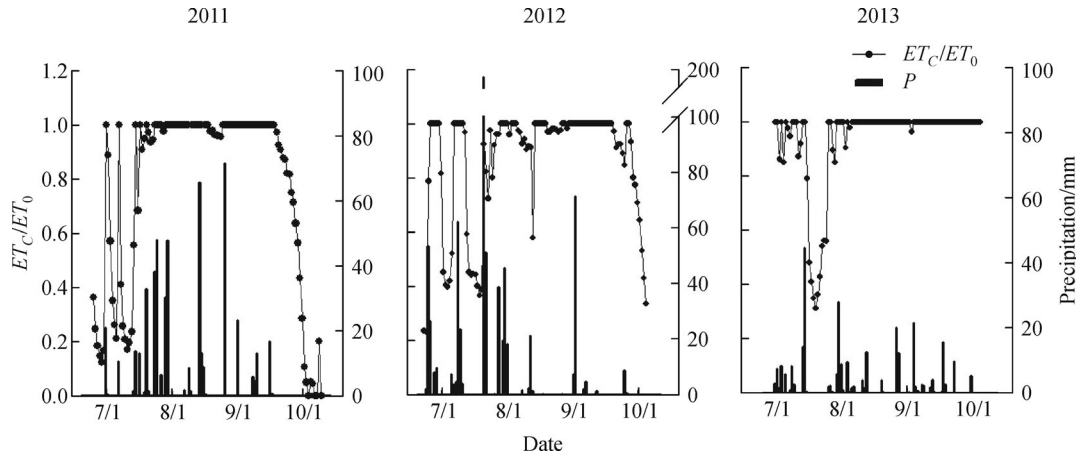


Fig. 6 Relationship between the ratio of actual daily evapotranspiration to the potential daily evapotranspiration ( $ET_C/ET_0$ ) and the precipitation in 2011, 2012, and 2013

Table 7 The soil water balance calculated for the entire summer maize growth period in 0–100 cm soil profile in 2011, 2012, and 2013

Year	Date	$\Delta SW/mm$	$P/mm$	$R/mm$	$D/mm$	$U/mm$	$ET/mm$	$E/mm$	$T/mm$
2011	(6.25–8.02)	123.80	266.70	43.30	0.00	14.30	113.90	88.40	25.50
	(8.02–8.29)	–33.40	83.10	0.00	0.00	0.00	116.50	8.00	108.50
	(8.29–9.22)	–19.60	64.00	0.00	0.00	0.00	83.60	4.10	79.50
	(9.22–10.10)	–31.10	0.20	0.00	0.00	0.00	31.30	0.20	31.10
	Whole growth period	39.70	414.00	43.30	0.00	14.30	345.30	100.70	244.60
2012	(6.23–7.18)	86.40	202.50	30.40	7.90	0.00	77.80	72.60	5.20
	(7.18–7.24)	94.60	238.60	100.30	27.90	0.00	15.80	10.90	4.90
	(7.24–8.14)	–25.60	126.10	23.70	56.70	0.00	71.30	12.40	58.90
	(8.14–8.27)	–66.20	1.30	0.00	15.50	0.00	52.00	1.10	50.90
	(8.27–9.12)	64.10	84.60	8.10	0.00	37.90	50.30	1.40	48.90
	(9.12–10.05)	–58.80	10.70	0.00	11.70	0.00	57.80	3.40	54.40
Whole growth period	94.50	663.80	162.50	119.70	37.90	325.00	101.80	223.20	
2013	(7.01–7.04)	13.00	11.60	0.00	0.00	14.90	13.50	13.50	0.00
	(7.04–7.17)	18.90	84.40	12.50	10.20	0.00	42.80	42.40	0.40
	(7.17–8.07)	–37.60	36.70	0.00	17.20	0.00	57.10	41.40	15.70
	(8.07–8.22)	1.10	28.80	0.00	0.00	22.00	49.70	7.90	41.80
	(8.22–9.12)	–4.40	67.80	1.30	5.00	0.00	65.90	4.60	61.30
	(9.12–10.05)	19.30	43.10	0.30	0.00	15.20	38.70	5.40	33.30
Whole growth period	10.30	272.40	14.10	32.40	52.10	267.70	115.20	152.50	

Note:  $\Delta SW$ , the change in the soil water storage during a given period (mm);  $P$ , precipitation (mm);  $R$ , runoff (mm);  $D$ , deep percolation beyond the root zone (mm);  $U$ , upward capillary rise into the root zone (mm);  $ET$ , evapotranspiration (mm);  $E$ , evaporation (mm);  $T$ , transpiration (mm).

was concentrated during the maize growth period, which was in the order of 2012 > 2011 > 2013. Similarly, surface runoff was in descending order 2012 > 2011 > 2013, and deep percolation also followed the same order. The maximum growth-season *ET* (345 mm) and *T* (245 mm) occurred in 2011, while their minimum counterparts (i.e., *ET*, 268 mm; *T*, 153 mm) were recorded in 2013. The overall results showed that *E* differed slightly during 2011 to 2013, but *T* in 2013 was 80 mm lower than that in 2011 and 2012. Consequently, *ET* in 2013 was the smallest of the three years.

*WP* (Hussain and Al-Jaloud, 1995) was calculated as the ratio of crop yield to actual *ET*, which was 2.66, 2.50, and 2.59 kg·m<sup>-3</sup> for 2011, 2012, and 2013, respectively.

## 4 Discussion

### 4.1 Water consumption, yield and water productivity

*ET* in 2013 was the lowest for the three years investigated and it was apparent that *T* is intimately associated with aboveground biomass and yield of maize (Fig. 2, Table 5). The results suggested that the lowest *T* in 2013 might be due to the lowest aboveground biomass and yield. Meanwhile, DAP in 2013 was the latest, hence the length of the growing period was the shortest for the three years (Table 3). As a result, water and heat required by maize growth decreased, and consequently the grain number and weight of maize decreased. *T* also decreased accordingly. These results were consistent with those of previous studies<sup>[52,81,82]</sup>.

Under non-irrigated conditions, water consumption may vary with yield and rainfall, but the linear relationship between consumptive water and crop yield remains unchanged. This conclusion was supported by Guo<sup>[83]</sup>. In spite of the fact that the lowest yield and water consumption was observed in 2013, *WP* was not the lowest. The delayed sowing date and shorter DAP may result in lower yield and *ET*, but the smaller yet more uniformly distributed rainfall and the consequent higher soil infiltration (effective rainfall) coincided more closely with water-required stages, leading to only a moderately low *WP*.

### 4.2 Climatic factors, depth of groundwater table and water productivity

Zhang<sup>[84]</sup> found that the average *WP* of maize for a long-term irrigation experiment during a 30-year period (1979–2009) in NCP was 1.72 kg·m<sup>-3</sup>. However, our simulation results showed that the average *WP* of rain-fed summer maize was 2.58 kg·m<sup>-3</sup> from 2011 to 2013 under non-irrigated conditions. The difference may be attributed to our field experiments on the piedmont plain of Yanshan Mountain, which has relatively plentiful groundwater and

a relatively shallow groundwater depth (1.0–1.5 m). Childs<sup>[85]</sup> and Yang<sup>[86]</sup> showed that crop water consumption and yield were very sensitive to change in groundwater depths, especially capillary rise during water-stress periods.

To investigate crop responses to long-term climatic factors, we also conducted a simulation by using a 30-year (1980–2010) historical climatic data set. In this long-term simulation, the required parameters by crop, soil, management, and initial water conditions by AquaCrop were set as the same as those in the three calibrated and validated years (2011–2013). We set two groundwater depths (i.e., one at 1.5 m where groundwater in our field experiments can recharge the crop in periods of water shortage, and the other where groundwater is deep enough so that capillary recharge is impossible in water shortage periods in most parts of the NCP) to examine the responses of crop yield and *WP* to differed water conditions, i.e., water-stress (Fig. 7), and no water-stress (Fig. 8).

Large variations in maize growth-season precipitation were observed over the 30 years, ranging from 163 mm to 712 mm. The results showed that soil moisture was replenished by timely capillary groundwater recharge received in dry years (e.g., 1999 and 2003, in which the growth-seasons rainfall were less than 200 mm) (Fig. 7). However, in cases of no capillary groundwater recharge (Fig. 8), soil water deficit led to the declining crop yield and *WP*. This can be further illustrated by the *WP* achieved in 1999 and 2003 under no water stress conditions, which was 2.49 and 2.24 kg·m<sup>-3</sup>, respectively (Fig. 7). In contrast, the *WP* under water stress conditions was only 1.92 and 1.97 kg·m<sup>-3</sup> (Fig. 8). Therefore, in dry years supplementary irrigation must be applied if a higher yield and *WP* is desired. It should also be noted that the above results of high yield and *WP* were achieved under the special condition of shallow groundwater depth. However, only part of the piedmont NCP has such favorable conditions, so irrigation will be necessary. Such irrigation, however, can be supplementary and relatively small compared to the growing-season rainfall, and would not affect the water balance of the region nor result in over-tapping groundwater. The analysis over a 30-year (1980–2010) of the water balance for rain-fed summer maize revealed that growing-season precipitation, *ET*, runoff and deep percolation were 379, 346, 35, and 79 mm, respectively, while the annual precipitation was 543 mm, suggesting that the annual precipitation can meet the water requirement of summer maize. Even in dry years, the rainfall also met most of the crop water requirement. However, if higher yield and *WP* was needed, supplementary irrigation would be necessary.

## 5 Conclusions

AquaCrop was calibrated and validated for summer maize

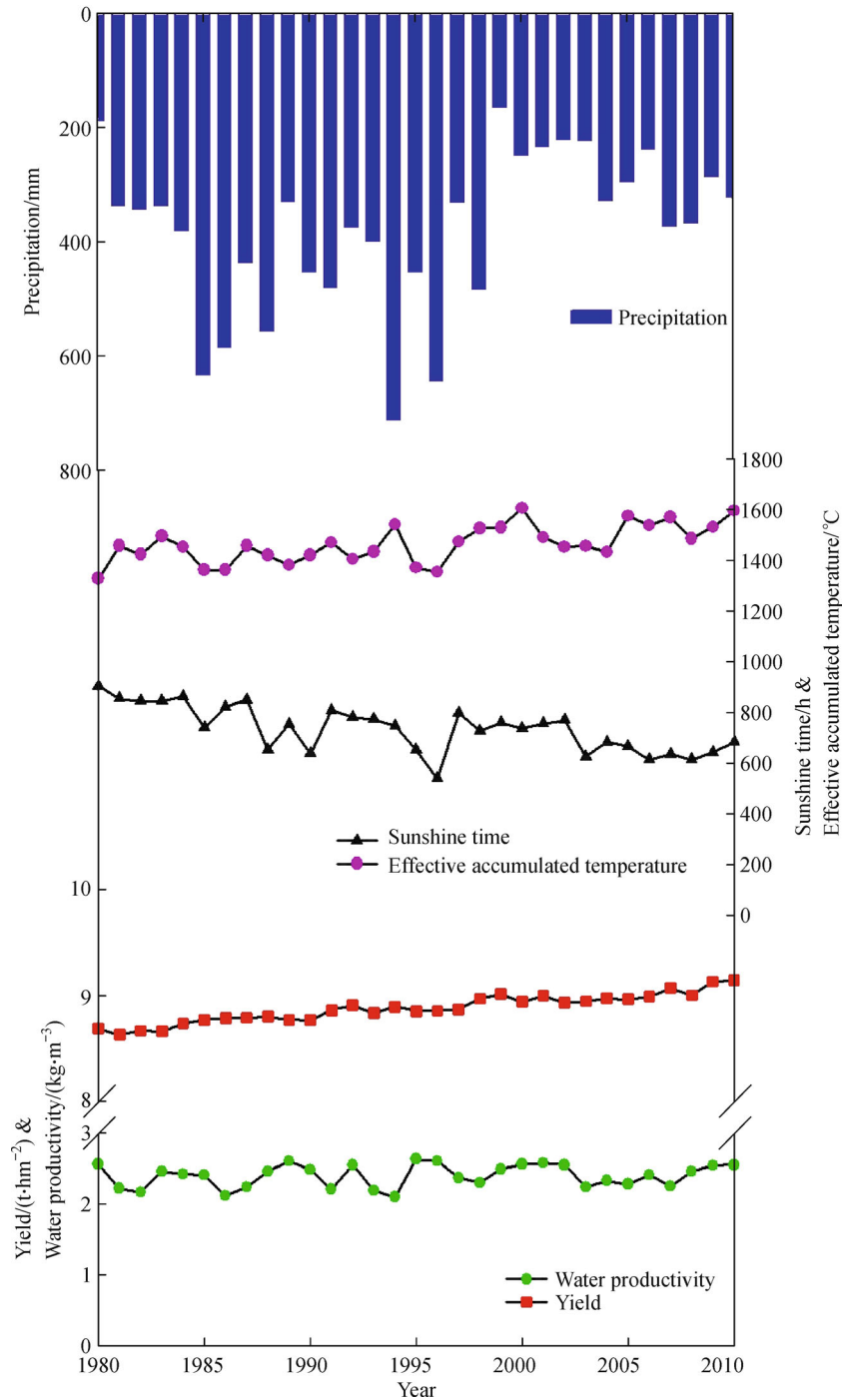
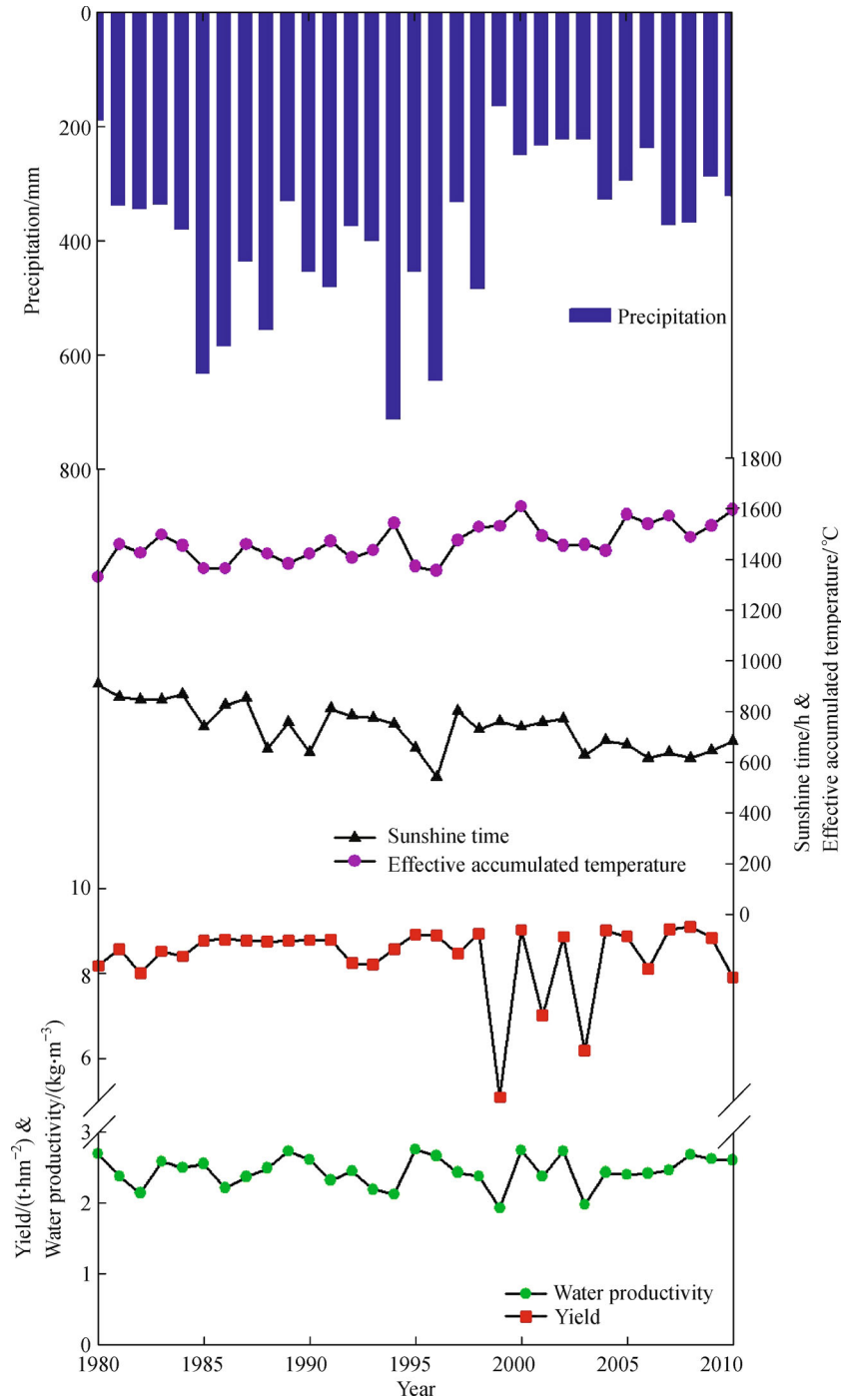


Fig. 7 The growth season precipitation, effective accumulated temperature, sunshine hours over the simulated period (1980–2010), and the simulated maize water productivity and yield under no water stress conditions (groundwater table = 1.5 m)

in the piedmont of NCP and the results suggested that it was appropriate for investigating crop biomass and yield, soil water storage in the root zone and the soil water balance. This research also indicated that rain-fed summer maize was a water-efficient crop and multiple-year *WP* could be as high as 2.58 kg·m<sup>-3</sup>, which was a fairly high *WP* for maize. Achievement of such a high level of *WP* in

this study may be partly attributed to capillary rise of water as a result of the shallow groundwater depth, which can also account for the sound ecosystem service functions maintained in the study area. More significantly, the results obtained from a long-term climate and varying groundwater depths (i.e., shallow, 1.0–1.5 m, and deeper) simulation suggested that a high *WP* might be achieved



**Fig. 8** The growth season precipitation, effective accumulated temperature, sunshine hours over the simulated period (1980–2010), and the simulated maize water productivity and yield under water stress conditions (groundwater table was as deep as possible)

in monsoonal dry years in areas with capillary groundwater as a result of shallow groundwater depths, however, in areas without such shallow groundwater depth, irrigation would be necessary. However, this kind of irrigation would not affect the water balance of NCP and not result in groundwater over-pumping if a single summer maize cropping system were adopted. The 30-year water balance on rain-fed summer maize suggested that the annual

precipitation can meet the water requirement of summer maize and even in dry years, the rainfall also met most of the crop water requirement. However, a higher yield and *WP* would also necessitate supplementary irrigation. Hence, the annual precipitation can meet both the consumptive water requirement of maize crop (i.e., rain-fed or rain-fed plus supplementary irrigation) and ecosystem services, thus a beneficial outcome for both

food security and ecosystem services can be assured.

**Acknowledgements** The authors are grateful for financial support provided by the IAEA (CRP14483) and China National Science and Technology Pillar Program (2012BAD05B02).

**Compliance with ethics guidelines** Jingjing Wang, Feng Huang, and Baoguo Li declare that they have no conflict of interest or financial conflicts to disclose.

This article does not contain any studies with human or animal subjects performed by any of the authors.

## References

- Du T S, Kang S Z, Zhang X Y, Zhang J H. China's food security is threatened by the unsustainable use of water resources in North and Northwest China. *Food and Energy Security*, 2014, **3**(1): 7–18
- Fu G B, Liu C M, Chen S L, Hong J L. Investigating the conversion coefficients for free water surface evaporation of different evaporation pans. *Hydrological Processes*, 2004, **18**(12): 2247–2262
- Fang Q X, Mab L, Green T R, Yu Q, Wang T D, Ahuj L R. Water resources and water use efficiency in the North China Plain: current status and agronomic management options. *Agricultural Water Management*, 2010, **97**(8): 1102–1116
- Liu W B, Fu G B, Liu C M, Song X Y, Ouyang R. Projection of future rainfall for the North China Plain using two statistical downscaling models and its hydrological implications. *Stochastic Environmental Research and Risk Assessment*, 2013, **27**(8): 1783–1797
- Sun H Y, Zhang X Y, Chen S Y, Pei D, Liu C M. Effects of harvest and sowing time on the performance of the rotation of winter wheat–summer maize in the North China Plain. *Industrial Crops and Products*, 2007, **25**(3): 239–247
- Fu G B, Charles S P, Yu J J, Liu C M. Decadal climatic variability, trends and future scenarios for the North China Plain. *Journal of Climate*, 2009, **22**(8): 2111–2123
- Li B G, Peng S Q. Chinese agricultural water report 1998–2007. Beijing: China Agriculture Press, 2009, 1–20 (in Chinese)
- Brown L. Who will feed China?—Wake-up call for a small planet. New York: W.W. Norton & Company, 1995
- Heilig G K, Fishcer G, van Velthuizen H. Can China feed itself?—An analysis of China's food prospects with special reference to water resources. *International Journal of Sustainable Development and World Ecology*, 2000, **7**(3): 153–172
- Huang F, Li B G. Assessing grain crop water productivity of China using a hydro-model-coupled-statistics approach. Part I: method development and validation. *Agricultural Water Management*, 2010, **97**(7): 1077–1092
- Wallace J S, Gregory P J. Water resources and their use in food production systems. *Aquatic Sciences*, 2002, **64**(4): 363–375
- Zhang J. China's success in increasing per capita food production. *Journal of Experimental Botany*, 2011, **62**(11): 3707–3711
- Wang P, Song X F, Han D M, Zhang Y H, Zhang B. Determination of evaporation, transpiration and deep percolation of summer corn and winter wheat after irrigation. *Agricultural Water Management*, 2012, **105**: 32–37
- Piao S, Ciais P, Huang Y, Shen Z, Peng S, Li J, Zhou L, Liu H, Ma Y, Ding Y, Friedlingstein P, Liu C, Tan K, Yu Y, Zhang T, Fang J. The impacts of climate change on water resources and agriculture in China. *Nature*, 2010, **467**(7311): 43–51
- Zhai P M, Pan X H. Change in extreme temperature and precipitation over Northern China during the second half of the 20th century. *Acta Geographica Sinica*, 2003, **58**(Supplement): 1–10 (in Chinese)
- Zhai P M, Zhang X B, Wan H, Pan X H. Trends in total precipitation and frequency of daily precipitation extremes over China. *Journal of Climate*, 2005, **18**(7): 1096–1108
- Li B G, Gong Y S, Zuo Q. Application of dynamic models in soil water. Beijing: Science Press, 2000, 1–199 (in Chinese)
- Matthews R B, Rivington M, Muhammed S, Newton A C, Hallett P D. Adapting crops and cropping systems to future climates to ensure food security: the role of crop modelling. *Global Food Security*, 2013, **2**(1): 24–28
- Soltani A, Hoogenboom G. Assessing crop management options with crop simulation models based on generated weather data. *Field Crops Research*, 2007, **103**(3): 198–207
- Vanuytrecht E, Raes D, Willems P. Global sensitivity analysis of yield output from the water productivity model. *Environmental Modelling & Software*, 2014, **51**: 323–332
- McCown R L, Hammer G L, Hargreaves J N G, Holzworth D P, Freebairn D M. APSIM: a novel software system for model development, model testing and simulation in agricultural systems research. *Agricultural Systems*, 1996, **50**(3): 255–271
- Ritchie J T, Godwin D C, Otter-Nacke S. CERES–Wheat: a simulation model of wheat growth and development. Texas: Texas A&M University Press, 1985
- Smith M. CROPWAT: a computer program for irrigation planning and management. Rome: FAO, 1992
- Raes D, Steduto P, Hsiao C, Fereres E. AquaCrop version 3.1 plus reference manual. Rome: FAO, 2011
- Wiyono K A, Kasomekera Z M, Feyen J. Effect of tied-ridging on soil water status of a maize crop under Malawi conditions. *Agricultural Water Management*, 2000, **45**(2): 101–125
- FAO. AquaCrop: the FAO crop-model to simulate yield response to water. <http://www.fao.org/nr/water/aquacrop.html>, 2010-10-1
- Farahani H J, Izzi G, Oweis T Y. Parameterization and evaluation of the AquaCrop model for full and deficit irrigated cotton. *Agronomy Journal*, 2009, **101**(3): 469–476
- Hsiao T C, Heng L, Steduto P, Rojas-Lara B, Raes D, Fereres E. AquaCrop: the FAO crop model to simulate yield response to water: III. Parameterization and testing for maize. *Agronomy Journal*, 2009, **101**(3): 448–459
- Raes D, Steduto P, Hsiao T C, Fereres E. AquaCrop: the FAO crop model to simulate yield response to water: II. Main algorithms and software description. *Agronomy Journal*, 2009, **101**(3): 438–447
- Steduto P, Hsiao T C, Raes D, Fereres E. AquaCrop: the FAO crop model to simulate yield response to water: I. Concepts and underlying principles. *Agronomy Journal*, 2009, **101**(3): 426–437
- Raes D, Steduto P, Hsiao T C, Fereres E. AquaCrop reference manual (Version 4.0). <http://www.fao.org/nr/water/aquacrop.html>, 2012-2-1
- Rankine D R, Cohen J E, Taylor M A, Coy A D, Simpson L A,

- Stephenson T, Lawrence J L. Parameterizing the FAO AquaCrop model for rain-fed and irrigated field-grown sweet potato. *Agronomy Journal*, 2015, **107**(1): 375–387
33. Sam-Amoah L K, Darko R O, Owusu-Sekyere J D. Calibration and validation of AquaCrop for full and deficit irrigation of hot pepper. *ARPN Journal of Agricultural and Biological Science*, 2013, **8**(2): 175–178
  34. Geerts S, Raes D, Garcia M, Taboada C, Miranda R, Cusicanqui J, Mhizha T, Vacher J. Modeling the potential for closing quinoa yield gaps under varying water availability in the Bolivian Altiplano. *Agricultural Water Management*, 2009, **96**(11): 1652–1658
  35. Andarzian B, Bannayan M, Steduto P, Mazraeh H, Barati M E, Barati M A, Rahnama A. Validation and testing of the AquaCrop model under full and deficit irrigated wheat production in Iran. *Agricultural Water Management*, 2011, **100**(1): 1–8
  36. Iqbal M A, Shen Y J, Stricevic R, Pei H W, Sun H Y, Amiri E, Penas A, Rio S D. Evaluation of the FAO AquaCrop model for winter wheat on the North China Plain under deficit irrigation from field experiment to regional yield simulation. *Agricultural Water Management*, 2014, **135**: 61–72
  37. Du W Y, He X K, Shamaila Z, Hu Z F, Zeng A J, Muller J. Yield and biomass prediction testing of AquaCrop model for winter wheat. *Transactions of the Chinese Society for Agricultural Machinery*, 2011, **42**(4): 174–178 (in Chinese)
  38. Li J, Fu C, Li S S, Zhang T N, Gu W R, Qiao T C, Xu W Z, Lu Y S, Wei S. The simulation for northeast spring wheat productivity based on the AquaCrop model and modeling verification. *Journal of Irrigation and Drainage*, 2014, **33**(2): 69–72 (in Chinese)
  39. Manasah S. Mkhabela, Paul R, Bullock. Performance of the FAO AquaCrop model for wheat grain yield and soil moisture simulation in western Canada. *Agricultural Water Management*, 2012, **110**: 16–24
  40. Farre I, Faci J M. Comparative response of maize and sorghum to deficit irrigation in a Mediterranean environment. *Agricultural Water Management*, 2006, **83**: 135–143
  41. Araya A, Keesstra S D, Stroosnijder L. Simulating yield response to water of Teff (*Eragrostis tef*) with FAO's AquaCrop model. *Field Crops Research*, 2010, **116**(1–2): 196–204
  42. Heng L K, Hsiao T, Evett S, Howell T, Steduto P. Validating the FAO AquaCrop model for irrigated and water deficient field maize. *Agronomy Journal*, 2009, **101**(3): 488–498
  43. Li H, Liu Y, Cai J B, Mao X M. The applicability and application of AquaCrop model. *Journal of Irrigation and Drainage*, 2011, **30**(3): 28–33 (in Chinese)
  44. Mebane V J, Day R L, Hamlett J M, Watson J E, Roth G W. Validating the FAO AquaCrop model for rain-fed maize in Pennsylvania. *Agronomy Journal*, 2013, **105**(2): 419–427
  45. Nyakudya I W, Stroosnijde L. Effect of rooting depth, plant density and planting date on maize (*Zea mays* L.) yield and water use efficiency in semi-arid Zimbabwe: modelling with AquaCrop. *Agricultural Water Management*, 2014, **146**: 280–296
  46. Zinyengere N, Mhizha T, Mashonjowa E, Chipindu B, Geerts S, Raes D. Using seasonal climate forecasts to improve maize production decision support in Zimbabwe. *Agricultural and Forest Meteorology*, 2011, **151**(12): 1792–1799
  47. Garcia-Vila M, Fereres E. Combining the simulation crop model AquaCrop with an economic model for the optimization of irrigation management at farm level. *European Journal of Agronomy*, 2012, **36**(1): 21–31
  48. Kiptum C K, Kipkorir E C, Munyao T M, Ndambuki J M. Application of AquaCrop model in deficit irrigation management of cabbages in Keiyo Highlands. *International Journal of Water Resources and Environmental Engineering*, 2013, **5**(7): 360–369
  49. Wellens J, Raes D, Traore F, Denis A, Djaby B, Tychon B. Performance assessment of the FAO AquaCrop model for irrigated cabbage on farmer plots in a semi-arid environment. *Agricultural Water Management*, 2013, **127**: 40–47
  50. Steduto P, Raes D, Hsiao T C, Fereres E, Heng L, Izzi G, Hoogeveen J. AquaCrop: a new model for crop prediction under water deficit conditions. *CIHEAM: Zaragoza Options Méditerranéennes-Series A*, 2008, 285–292
  51. Doorenbos J, Kassam A H. Yield response to water. *FAO Irrigation and Drainage Paper No. 33. Rome, Italy*, 1979
  52. de Wit C T. Transpiration and crop yields. The Netherlands: *Wageningen University*, 1958, 1–88
  53. Hanks R J. Yield and water-use relationships: an overview, Ch. 9. In Taylor H.M., Jordan W.R., Sinclair T.R. Limitations to efficient water use in crop production. *ASA, CSSA, SSSA, Madison, WI*, 1983, 393–411
  54. Tanner C B, Sinclair T R. Efficient water use in crop production: research or re-search? Ch. 1. In H.M. Taylor, W.R. Jordan, and T.R. Sinclair (ed.). Limitations to efficient water use in crop production. *ASA, CSSA, and SSSA, Madison, WI*, 1983, 1–27
  55. Steduto P, Hsiao T C, Fereres E, Raes D. Crop yield response to water. [http://www.fao.org/docrep/016/i2800e/i2800\\_e00.htm](http://www.fao.org/docrep/016/i2800e/i2800_e00.htm), 2012-12-1
  56. Idso S B, Reginato R J, Jackson R D, Kimball B A, Nakayama F S. The three stages of drying of a field soil. *Soil Science Society of America Journal*, 1974, **38**(5): 831–837
  57. Rallison R E. Origin and evolution of the SCS runoff equation. New York: *ASCE*, 1980, 912–924
  58. Steenhuis T S, Winchell M, Rossing J, Zollweg J A, Walter M F. SCS runoff equation revisited for variable-source runoff areas. *Journal of Irrigation and Drainage Engineering*, 1995, **121**(3): 234–238
  59. USDA. Estimation of direct runoff from storm rainfall. National Engineering Handbook, *Washington DC, USA. Section 4 Hydrology, (Chapter 4)*, 1964, 1e24
  60. Raes D. A summary simulation model of the water budget of a cropped soil. Leuven: *Katholieke Universiteit Leuven University*, 1982, 1–110
  61. Raes D, Lemmens H, Van Aelst P, Van den Bulcke V, Smith M. IRIS: irrigation scheduling information system. Leuven: *Department of Land Management*, 1988, 1: 1–199
  62. Raes D, Geerts S, Kipkorir E, Wellens J, Sahli A. Simulation of yield decline as a result of water stress with a robust soil water balance model. *Agricultural Water Management*, 2006, **81**(3): 335–357
  63. Janssens P. Invloed van eenondiepe grondwatertafel op de planning van irrigaties voorintensieve-groenteteelt. Dissertation for the Master Degree. Leuven: *K. U. Leuven University*, 2006
  64. Belmans C, Wesseling J G, Feddes R A. Simulation of the water

- balance of a cropped soil: SWATRE. *Journal of Hydrology*, 1983, **63**(3-4): 271–286
65. Feddes R A, Kowalik P J, Zaradny H. Simulation of field water use and crop yield. *Simulation Monographs, Pudoc, Wageningen, Centre for agricultural publishing and documentation, the Netherlands*, 1978
  66. Hoogland J C, Belmans C, Feddes R A. Root water uptake model depending on soil water pressure heads and maximum water extraction rate. *Acta Horticulturae*, 1981, **119**(119): 123–135
  67. Philip J R. Evaporation, and moisture and heat fields in the soil. *Journal of Meteorology*, 1957, **14**(4): 354–366
  68. Ritchie J T. Model for predicting evaporation from a row crop with incomplete cover. *Water Resources Research*, 1972, **8**(5): 1204–1213
  69. Adams J E, Arkin G F, Ritchie J T. Influence of row spacing and straw mulch on first stage drying. *Soil Science Society of America Journal*, 1976, **40**(3): 436–442
  70. Villalobos F J, Fereres E. Evaporation measurements beneath corn, cotton, and sunflower canopies. *Agronomy Journal*, 1990, **82**(6): 1153–1159
  71. Allen R G, Pereira L S, Raes D, Smith M. Crop evapotranspiration: guidelines for computing crop water requirements. *Irrigation and Drainage Paper no. 56*. Rome: FAO, 1998, 1–300
  72. Steduto P, Hsiao T C, Fereres E. On the conservative behavior of biomass water productivity. *Irrigation Science*, 2007, **25**(3): 189–207
  73. Klute A, Dirksen C. Hydraulic conductivity and diffusivity: laboratory methods. In: Klute A, ed, *Methods of soil analysis. Part 1: physical and mineralogical methods*, 2nd ed. ASA, WI, 1986, 687–732
  74. Klute A. Water Retention: Laboratory Methods. In: Klute A, ed. *Methods of soil analysis. Part 1: physical and mineralogical methods*, 2nd edn. ASA, WI, 1986, 635–660.
  75. Blum A. Drought resistance, water-use efficiency, and yield potential—are they compatible, dissonant, or mutually exclusive? *Australian Journal of Agricultural Research*, 2005, **56**(11): 1159–1168
  76. Hatfield J L, Sauer T J, Prueger J H. Managing soils to achieve greater water use efficiency: a review. *Agronomy Journal*, 2001, **93**(2): 271–280
  77. Hussain G, Al-Jaloud A A. Effect of irrigation and nitrogen on water use efficiency of wheat in Saudi Arabia. *Agricultural Water Management*, 1995, **27**(2): 143–153
  78. Sinclair T R, Tanner C B, Bennett J M. Water-use efficiency in crop production. *Bioscience*, 1984, **34**(1): 36–40
  79. Willmott C J. Some comments on the evaluation of model performance. *Bulletin of the American Meteorological Society*, 1982, **63**(11): 1309–1313
  80. Kat C J, Els P S. Validation metric based on relative error. *Mathematical and Computer Modelling of Dynamical*, 2012, **18**(5): 487–520
  81. Early E B, McIlrath W O, Seif R D, Hageman R H. Effects of shade applied at different stages of plant development on corn (*Zea mays*) production. *Crop Science*, 1967, **7**(2): 151–156
  82. Xue Q Y, Wang J, Cao X P, Ma W, Feng L P. Effect of sowing date and variety on growth and population characteristics of summer maize in North China Plain. *Journal of China Agricultural University*, 2012, **17**(5): 30–38 (in Chinese)
  83. Guo Q F, Wang Q C, Wang L M. China maize cultivation. Shanghai: Shanghai Science and Technology Press, 2004, 462–480 (in Chinese)
  84. Zhang X Y, Chen S Y, Sun H Y, Shao L W, Wang Y Z. Changes in evapotranspiration over irrigated winter wheat and maize in North China Plain over three decades. *Agricultural Water Management*, 2011, **98**(6): 1097–1104
  85. Childs E C. The nonsteady state of the water table in drained land. *Journal of Geophysical Research*, 1960, **65**(2): 780–782
  86. Yang Y H, Masataka W, Zhang X Y, Hao X H, Zhang J Q. Estimation of groundwater use by crop production simulated by DSSAT-wheat and DSSAT-maize models in the piedmont region of the North China Plain. *Hydrological Processes*, 2006, **20**(13): 2787–2802